Title: Mosaic evolution, constraint, and constructional opportunity in great apes

Author: Caroline Parins-Fukuchi*[1]

[1]Department of Ecology and Evolutionary Biology, University of Michigan, Ann Arbor, MI, USA 48109

*Author for correspondence: cfukuchi@umich.edu

Abstract: Researchers often seek adaptive explanations for macroevolutionary patterns in phenotypic diversification. Although there is substantial evidence for the potency of environmental pressures in driving evolutionary change, the role of constructional factors, which include functional and developmental constraints, has been examined less thoroughly. Using a dataset of 149 quantitative skeletal traits sampled from the cranium, forelimb, and pelvis representing 10 extant and 9 fossil haplorrhine taxa, I recovered five character suites, revealing distinct patterns in macroevolutionary disparity throughout the Miocene. Comparison to encephalization and neurological developmental traits revealed further support for a general pattern in evolutionary and developmental flexibility shared by all great apes. These analyses contribute to a view of ape evolution that is defined by episodic bursts in phenotypic innovation that have built a wide array of functional diversity over a foundation of shared developmental and anatomical structure that was laid throughout the Miocene. Notably, much of humans' phenotypic distinctiveness can be explained by earlier shifts in morphological evolution and integration. Jointly considering the analyses of skeletal and developmental traits suggests that an early increase in developmental flexibility in apes was met with rapid canalization into distinct functional suites.

Keywords: hominoidea, mosaic evolution, integration, Miocene

Introduction

Identification of the adaptive drivers of evolutionary change has long been a central research program in paleontology and comparative biology. Researchers often seek specific environmental and ecological patterns that can explain both rapid morphological innovation and lineage diversification. For example, many comparative studies seek to identify correlations between macroevolutionary diversification and the emergence and colonization of new ecological niches. Many of these studies have found that shifts in the evolutionary rate of phenotypic characters, such as body size, coincide with those in ecological traits, such as climatic variables and biogeography (Harmon et al., 2003, Losos et al., 2006, Mahler et al., 2013, Slater and Friscia 2018). There is also evidence in some taxa that elevated rates of phenotypic evolution may sometimes correspond to elevated rates of lineage diversification (Rabosky et al. 2013, but see Crouch and Ricklefs 2019).

The early focus on environmental adaptation was first codified through the conceptual application of modern synthesis-era population genetic theory to questions at the macroevolutionary scale. George Gaylord Simpson combined the quantitative descriptions of selection, drift, and fitness landscapes developed during the synthesis to suggest that large evolutionary changes occur rapidly as species move between and optimize their position within ‘adaptive zones’ shaped by ecology. In this illustration, each zone is represented as an adaptive peak on a multi-dimensional fitness landscape, each of which describes a locally optimal combination of phenotypes. Although initially maintaining position on a single peak due to stabilizing selection, Simpson hypothesized

that genetic drift may cause species to descend and cross adaptive valleys, during which positive selection re-emerges to propel the species to a new peak. This image has been influential, providing the theoretical basis for major evolutionary concepts. For example, large evolutionary radiations are often hypothesized be limited in their intensity by the availability of new ecological opportunities through environmental changes or improvement of competitive ability (Rainey and Travisano 1998, Yoder et al., 2010, Wagner and Harmon et al 2012, but see Slater 2015).

The role of ecological processes in generating morphological novelty can be contrasted with an increasing focus on constructional factors, such as developmental (Gould and Lewontin 1979, Olson 2012) and selective (Charlesworth et al., 1982, Cheverud 1984, Maynard-Smith et al., 1985) constraints in shaping macroevolutionary patterns. Developmental constraint occurs when phenotypes are linked in ontogeny. When traits are developmentally linked, but functionally autonomous, the available set of selectively advantageous modifications belonging to one is limited by the fitness effect on the other. Selective constraint exists when multiple traits contribute to a shared function that is under selection. Although any particular trait may perform many functions that contribute to fitness in different ways, the phenotype for each trait that contributes to a shared function that is under strong selection will be limited to values that facilitate its contribution alongside the other constituent traits. Developmental constraints and selection can generate similar patterns by causing the formation of modules of characters that are linked in their evolutionary trajectories through a descriptive process traditionally referred to as ‘integration’ (Olson and Miller 1958).

Constructional factors can influence evolution in significant ways. For example, when ecological opportunity is abundant, evolutionary radiations can be driven primarily by the release of constraints (Wagner et al. 2003). Canalization of phenotypic variation through development can facilitate rapid adaptive evolution (Wagner 1988). Reductions in developmental constraint can also shape macroevolutionary patterns by driving increases in evolutionary rate (Donoghue and Ree 2000). This pattern appears to hold for integration more generally, with higher degrees of integration often linked to lower evolutionary disparity and rate (Goswami et al. 2014, 2015). The set of evolutionary limitations imposed by integration through development and selection are crucial in determining the capacity for a clade to diversify phenotypically. Together, these factors might be said to determine the level of 'constructional opportunity' available at a given time. While the amount of ecological opportunity is often evoked as a primary driver in the emergence of evolutionary novelty, constructional opportunity may also act as a limiting factor by restricting the range of possible adaptations available to a population faced with ecological pressure.

Apes have been extensively studied in the context of both developmental constraint and environmental adaptation. Young et al. (2010), hereafter referred to as YEA, found that apes display low functional and developmental integration between the fore- and hindlimb in comparison to cercopithecines. Reduced integration can confer greater functional flexibility, and so may have facilitated the proliferation of the diverse locomotor function across living and fossil apes. Changes in developmental timing have also been important in ape evolution. Developmental heterochrony appears to have driven

the emergence of many key aspects of hominin morphology in the cranium and post-cranium (Gould 1977, Berge 1998). This long-standing interest in the developmental basis of ape evolution has not excluded environmental hypotheses. Environmental fluctuations throughout the Miocene and Pliocene have also frequently formed the basis for adaptive hypotheses across apes (Andrews 1992, Ruff 1994, Michel et al., 2014). The body plans of hominins, and undoubtedly apes in general, have been shaped through modifications to separate suites of traits occurring at different times (Holloway 1973, McHenry 1975). These diverse threads suggest that a multiplicity of causes, perhaps including both ecological opportunity and constructional factors, has shaped the evolution of hominoid body plans. As a result, apes are an excellent candidate taxon in which to pluralistically examine the mosaic patterns in constraint and innovation that have shaped living and fossil vertebrate body plans.

In this study, I sought to examine whether the increased developmental flexibility in body plan shared by great apes corresponds to an increase in constructional opportunity that is associated with elevated rates of evolutionary disparification in morphological and neurological traits across all apes. To address these questions, I reconstructed the mosaic macroevolutionary patterns in morphological, neurological, and developmental phenotypes across living and fossil great apes throughout the Miocene. To better understand these empirical results, I also present a set of simulations to generate a theoretical expectation for the patterns in disparity expected when Markovian diffusion is constrained by both selection and development. Taken together, these analyses suggest

the capability for shifting patterns in constraint to create constructional opportunities that generate repeated and dramatic episodes in morphological innovation.

Methods

Morphological data

I gathered a dataset of 149 quantitative morphological traits from the literature (Lewton 2010, Worthington 2012) spanning the cranium, forelimb, and pelvis. These traits were sampled across 10 extant taxa. I also collected fossil cranial and forelimb traits from Worthington (2012), retaining all taxa with at least 25% matrix occupancy. Taxa were all studied at the generic level, with each extant genus represented by a single exemplar species. Each morphological trait represented a dimensionless ratio or geometric mean. I scaled the traits to display an empirical variance of 1 across all taxa. This simplified the analyses by reducing the complexity of the dataset, while retaining the same comparative information. Since the original traits were dimensionless, both the unscaled and the scaled datasets would facilitate examination of *relative*, rather than absolute, evolutionary rates, but the scaled traits improve Markov-chain Monte Carlo (MCMC) mixing and simplify the identification of mosaic suites.

Neurological data

To directly study the evolutionary patterns in related developmental and phenotypic traits, I also gathered neurological data from the literature (Capellini et al., 2010, Boddy et al., 2012). For neurological phenotype, I collected encephalization quotients (EQ) estimated in 76 primate species by Boddy et al. (2012). EQ is calculated by fitting a nonlinear model to brain size and body size and taking the deviations

(residuals) from the best fit curve and so measures the enlargement of brain size while controlling for allometry with body size. I compared EQ patterns to those in a postpartum encephalization development (ED) metric calculated as:

$$ED = EQ_{adult} - EQ_{neonatal} \quad (1)$$

ED is therefore intended to reflect the amount of brain tissue grown by members of each species following birth relative to their body size. Neonatal brain and body mass data representing 24 primate species were acquired from Capellini et al. (2010).

Fossil placement and divergence time estimation

Since the evolutionary relationships between the extant taxa represented in the morphological dataset have all been extensively studied and are well-resolved, I used these as a fixed scaffolding to place the fossil taxa. Fossil placements were inferred from the continuous trait dataset using the cophymaru program (Parins-Fukuchi 2018). I used the 'binary weights' procedure to filter out reliable traits from ones likely to mislead by using the extant tree as a fixed point of reference. Markov-chain Monte Carlo (MCMC) simulations were run for 1,000,000 generations and checked manually for convergence. The posterior tree sample was summarized as the maximum clade credibility tree using sumtrees.py (Sukumaran and Holder 2010).

For downstream comparative analyses, I also estimated divergence times on the full 19-taxon tree. I downloaded cytochrome B sequences from Genbank representing each of the 10 extant taxa. Molecular dating was performed using Beast version 2.4.8 (Bouckaert et al. 2014) using the fossilized birth-death prior. The topology was fixed to

the summary tree generated during the fossil placement step. Temporal occurrence ranges for the fossil taxa were assembled from the literature.

Evolutionary rates across mosaic morphological suites

I used the *greedo* program to recover mosaic patterns in disparity from the continuous trait dataset (Parins-Fukuchi 2018). *Greedo* is a phylogenetic clustering/mixture model estimation approach that uses the Akaike information criterion (AIC) to iteratively merge and split clusters of traits to find a best-supported set of character suites based on shared patterns in disparity, where each is represented by a tree with branch lengths. This process recovers an estimate of the number of suites, the membership for each trait, and a tree with branch lengths scaled to units of disparity for each suite. Fossil taxa were not included in the mosaic analyses, because they were too fragmentary in their sampling to inform disparity patterns when the traits were split into suites. I performed many runs of the *greedo* procedure to avoid presenting results obtained from a suboptimal peak on the likelihood surface. Since several of the top clusterings yielded close AIC support, I performed an additional model-averaging step using Akaike weights to summarize the results as a graph where each trait occupies a node, and each link is weighted to reflect the total weighted AIC support across all the models. Comparative analyses were performed using a single summary clustering that resulted from application of the Markov clustering (MCL) algorithm to the support network (Dongen 2000).

To examine the anatomical composition of the mosaic suites of traits, I performed a statistical enrichment procedure to identify skeletal regions that were over and under-

represented in each suite relative to the proportions for each present in the entire dataset. The proportion of the 149-trait dataset represented by each skeletal region was used to generate a set of ‘expected’ values. I then compared these to the observed proportions within each suite to examine trends in the deviations of the proportions occupied by each region. I did not assess the statistical significance of these deviations, because 1) my aim was to examine the general patterns in the composition of each character suite rather than to determine absolute significance, and 2) the small sample size of the dataset generated expected chi-square test statistic values that were nearly entirely <5, making the test inappropriate. To examine the relative contributions of separate anatomical regions in shaping the macroevolutionary patterns reconstructed in each suite, I also performed a principal component analysis (PCA) on the traits contained within each suite. I then transformed the loadings to calculate the total variance contributed by each trait across all axes of the PCA, summing them to produce the contribution of each anatomical region.

I transformed the branch lengths for each mosaic suite, which were scaled to reflect disparity (total variance, *v*, accumulated over time *t*), to rates (*v* per unit *t*) using the results from the divergence time analysis. I also calculated evolutionary rates averaged over the entire morphological dataset while including the fossil taxa to coarsely reconstruct evolutionary tempo throughout the Miocene. Although this step missed valuable information recovered by the mosaic analyses, including the fossil taxa in this manner enabled finer resolution into the coarse patterns in evolutionary tempo throughout the Miocene.

Evolutionary rates in neurological data

I estimated macroevolutionary rates across primates in ED and EQ using BAMM version 2.5.0 (Rabosky 2014). Since the trees that I constructed for the morphological analysis contained only a fraction of the taxa present in the neurological datasets, I used the dated primate supertree packaged in BAMM that was originally sourced from Mos and Mooers (2006) and pruned the tips to match the taxa present in each dataset. MCMC simulations were run until the estimated sample size (ESS) well exceeded 200 for each parameter. Results were presented by plotting the mean rate estimated along each branch and the maximum *a posteriori* configuration of rate shifts using BAMMtools version 2.5.0 in R (Rabosky et al., 2014).

Simulated Markovian diffusion

To examine the expected effect of constructional opportunity stemming from both developmental constraint and selection on phenotypic evolution, I designed a set of evolutionary simulations based on a simple Markovian diffusion. In this system, quantitative traits belonging to a single population of organisms evolve stochastically along a fitness landscape. Each generation, values for each trait are proposed. Values that increase the overall fitness of the population are accepted. To mimic the effect of drift, values that decrease fitness are also accepted with some (user-specified) probability. Developmental constraint can be mimicked by proposing values for traits that covary, while selective constraints are modeled by evolving traits along a shared, multivariate adaptive landscape, modelled here using a mixture of multivariate Gaussian distributions. In a completely unconstrained system, each trait is evolved according to its own

univariate landscape, with its value drawn independently of all others in each generation. The script used to generate these simulations is available in the data supplement.

Results and Discussion

Composition of mosaic suites

The analysis of mosaic disparity recovered five suites of traits (Fig 1a). The cranium was the largest contributor of both traits and variance across all suites except for C4, which was represented by the pelvis alone (Fig. 1b and 1c). This reflects the higher sampling of cranial traits in the dataset. While the cranium has previously been shown to display substantial modularity (Felice and Goswami 2017), the results here suggest that individual cranial modules may result from the formation of broader evolutionary complexes shared with the post-cranium. The suites were distinct in their composition across postcranial anatomy: C0 was represented strongly by the wrist, ulna, and humerus; C1 was represented postcranially by the scapula; C2 by wrist and pelvic traits. The cranium was represented even more strongly than expected in C3 and contributed nearly half of the variance (Fig. 1b).

Rates of morphological evolution

The phylogenetic rate calculations for each suite revealed a strong pattern of evolutionary mosaicism (Fig. 1a). Three of the suites, C0, C1, and C3, displayed the highest rates after the divergence of the great apes from hylobatids, but prior to the divergence of gorillas from humans and chimpanzees. The two suites that did not experience the shared great ape rate increase, C2 and C4, experienced large bursts in *Homo*. This finding is consistent with general knowledge of human evolution, as both

suites are dominated by cranial traits and pelvic traits related to birthing and locomotor function (Table S1).

The rate analyses show that humans have experienced major macroevolutionary bursts. However, these are built over an anatomical structure shared by all great apes that was shaped in the Miocene during similarly dramatic episodes. For example, although suite C0 increased in evolutionary rate along the human branch, its evolution was shaped by a sustained period of elevated rate between 20 and 10 million years ago. This suggests that much of the 'groundwork' underlying the derivation of humans' unique features may predate the divergence between our lineage and chimpanzees'. The mosaic analysis also demonstrates that substantial visible phenotypic novelty can result from the evolutionary remodeling of a fairly small subset of the anatomy. The most elevated evolutionary rates in humans were observed in suites C2, C3, and C4, which cumulatively comprise fewer than one-third of the traits sampled in the matrix (Table S1). C4, the smallest suite (10 traits) displayed by far the largest increase in rate along the *Homo* lineage. Perhaps notably, C4 also was the most static character suite throughout the earlier stages in the hominoid radiation. Although enumerating characters does not itself constitute a particularly compelling independent line of evidence from which to interpret macroevolutionary trends, the mosaic pattern recovered here does suggest that the subset of biological variation unique to the human body plan is fairly small in comparison to the wide spectrum of evolutionary variance accumulated throughout ape evolution.

While the large amounts of missing data among the fossil taxa made an additional mosaic analysis infeasible, their inclusion revealed an otherwise hidden shift in

evolutionary rate that occurred at the root of hominoidea. The fossil data also recapitulated the burst in evolutionary rate during the mid-Miocene that was displayed by C0 and C1 in the mosaic analysis (Fig. 1 and 2). When averaging over all the traits and including fossil taxa, these two episodes are the most dramatic macroevolutionary events when tracing the evolutionary lineage leading to *Homo*, suggesting the importance of early shifts in the ape body plan in shaping the functional morphologies of living taxa.

Rates of neurological evolution

As with morphology, all great apes appear to have differentiated rapidly from other catarrhines in both EQ and ED. *Homo* displays the highest rate of both EQ and ED evolution. However, the human rate shift in both traits occurred as part of an older trend of rapid neurological evolution in African apes. For EQ, humans experienced a substantial increase in evolutionary rate relative to the rest of the African apes, despite the statistical evidence for a shared rate shift at the root of the clade (Fig. 3b). The shared macroevolutionary regime shared by all African apes is most apparent in encephalization development (Fig. 3a), where the estimated evolutionary rate in *Homo* increased only slightly after splitting from *Pan* (Fig. 3c). It appears that the increased encephalization developed throughout the post-natal period in humans reflects a general trend among great apes in the evolutionary plasticity of neurological development. As a result, the ability to develop a relatively large mass of brain tissue does not itself appear to be a strong limiting factor in the evolution of large encephalization in humans. Instead, the morphological analyses suggest that pelvic traits (C4 in Fig. 1) may have demanded a more dramatic alteration in macroevolutionary regime.

Structural and ecological opportunity in ape evolution

The elevated evolutionary rates experienced by apes early in their divergence may correspond to a general relaxation of developmental constraints in late Oligocene stem and ancestral hominoids. The burst in the evolutionary rate of neurological developmental traits discovered here and the reduced skeletal integration discovered by YEA both correspond in timing to the elevated rates in morphological evolution observed in most of the skeletal characters examined here (Fig. 1 and 2). Freed from previous developmental limitations, ape body plans would have rapidly diversified when placed in the context of the repeated environmental fluctuations that occurred throughout the mid and late Miocene (Michel et al. 2014, Hunt 2016) before becoming functionally canalized through development and stabilizing selection. This pattern is consistent with a scenario in which morphological features evolve by stochastic diffusion on a Simpsonian adaptive landscape that is alternately dampened and released by relaxed and shifting patterns in character integration.

Rapid and frequent environmental fluctuations throughout the Miocene suggest an abundance of theoretically available adaptive zones during the evolution of both cercopithecoids and hominoids. Paleoecological information extracted from deposits containing key hominoid taxa are so variable that environmental turnover often outpaces the effects of time-averaging (Michel et al. 2014). Early Miocene ape and monkey species evolved in often overlapping environmental conditions and shared similar ecomorphological and dietary habits. However, as their lineages diverged, apes evolved a diverse set of locomotor suites, while evolution in locomotor features has remained

comparatively static across old world monkeys (Hunt 2016). The patterns in developmental and mosaic morphological evolution revealed here suggest that the substantial differences between the two taxa in phenotypic disparity were shaped more by differences in patterns in integration and constraint rather than from the ecological opportunities available to either. While hominoids and cercopithecoids inhabited a similar range of habitats throughout their evolution, and so likely experienced a similar abundance of ecological opportunity, greater constructional opportunity is a distinguishing feature that correlates with hominoids' vast disparity in skeletal morphology.

The scenario entertained here for apes is consistent with recent work that suggests that the initial burst in phenotypic disparity that often accompanies the origin of a new lineage can result from an early relaxation of constraints through the dissolution of integrated modules that is followed by reformation of character suites that lead to rapid, correlated evolutionary changes between constituent characters (Wagner 2018). In the cited work, the author distinguishes this 'breakup-relinkage' model with one where evolutionary rates are elevated by a relaxation of constraint alone. Although in this study, I have focused most of the discussion on the relaxation of constraints, I should note that the formation of mosaic character suites and their distinct evolutionary patterns imply a strong pattern of integration within apes. Therefore, the recanalization of functional variation into a set of suites with distinct functional and developmental properties early in hominoid variation is likely equally important to the initial relaxation in constraint in having driven the remarkable morphological disparity observed across hominoid species.

Enablers in ape evolution

Bursts in phenotypic change and diversification are often preceded by evolutionary enablers that facilitate the construction of more diverse morphological forms or fulfill a necessary condition for the later emergence of a more derived trait (Gould 1977, Gould and Vrba 1982, Donoghue 2005). The evolution of developmental, morphological, and behavioral traits is often hierarchical through functional inter-dependencies and temporally autocorrelated, with changes in traits at relatively lower levels 'setting the stage' for higher-level traits by providing the developmental or structural conditions necessary for their emergence. The stepwise macroevolutionary bursts observed here show that hominoid evolution has been defined by sequential, episodic releases in constraint that likely set the stage for later innovations that compounded upon earlier constructional rearrangements.

Traits representing the neurocranium and pelvic aperture provide a straightforward example. Suites C2 and C3 from the morphological analysis, represented disproportionately by the cranium, experienced an initial burst in evolutionary rate along the branch leading to humans and chimpanzees. This was then followed by an additional burst in *Homo*. Likewise, EQ and ED have been evolving rapidly throughout the ape radiation, with ED experiencing an initial substantial increase in evolutionary rate prior to the splitting of chimps and humans (Fig. 3c). Although humans' extreme neurologic phenotypes stand out, these analyses demonstrate that they emerged within a backdrop of exceptional developmental flexibility in neurological traits shared by all great apes.

The initial burst in the rate of neurological developmental evolution along the MRCA branch of chimps and humans is mirrored in the two suites of skeletal traits that represent separate neurocranial and cranio-pelvic traits, C2 and C3. Although this pattern demands more detailed exploration with more resolute data, I speculate that the initial bursts in ED and suite C2 and C3 evolution may have provided a set of structural rearrangements that facilitated, at least in part, the later emergence of human-specific neurological and cognitive features. This scenario in part echoes the results of Rice (1998), who demonstrated that humans and chimpanzees both inherited a shared 'additional' stage of brain development from our most recent common ancestor. It is therefore possible that chimpazees possess more of the neurological groundwork that contributed to the evolution of humans' particular mode of cognition than has previously been appreciated.

Constrained Markovian diffusion and entropy

The patterns in character disparity shown here evoke a Markovian diffusion that is dampened by constructional limitations. The tightly integrated nature of vertebrate body plans suggests major constraints in their ability to fill morphospace. However, the pattern displayed by apes suggests that the integration of form may sometimes shift, allowing diffusion into new areas. Morphological evolution might then be conceived as a multivariate diffusion in morphospace where movement is directionally biased due to fitness differences modelled by a traditional Simpsonian adaptive landscape and certain regions are rendered inaccessible by structural interactions between characters. Although this diffusive model, including the feedback links between phenotype, development, and

environment, has been considered previously (Fisher 1986), its behavior has not been well-explored.

The results of the Monte Carlo simulations shed light on the empirical analyses by capturing the dynamics of a simplified integrated evolutionary system (Fig. 4). As is expected from quantitative genetic theory (Cheverud 1984, Maynard-Smith et al. 1985), developmental and selective constraints can generate similar patterns (Fig. 4a and 4b). In all these cases, the overall entropy observed in the system over time remains low, with the system tending to become stuck or moving away very slowly from a suboptimal location (Fig 4c and 4e) or crawling slowly in concert along a gradient (Fig 4a and 4b). However, when both selective and developmental constraints are released, the system displays high entropy, with each trait able to independently and rapidly jump between peaks (Fig. 4d). Such unconstrained movement would be expected to result in higher phenotypic disparity across clades by freeing individual lineages to generate novel character combinations that are distinct from one another either due to adaptation in distinct environments or stochastic differences in the sorting of variation.

The empirical analyses display similar patterns to the less constrained simulated diffusions. Alternation between patterns of integrations explored in the simulations would likely generate substantial novelty through the relaxation (Fig. 4c) and selective fixation (Fig. 4a) of constraints. Episodes of reduced developmental constraint (Fig. 3a) may have generated an initial burst of constructional opportunity that lead to rapid morphological diversification as ape populations were exposed to highly variable environments throughout the mid-Miocene. Under the evolutionary models explored here and

elsewhere (Wagner 2018), stabilizing effects such as developmental canalization (Waddington 1959) or selective covariance (Cheverud 1984) would then be expected to re-constrain the newly divergent phenotypes after an initial burst in disparification. This dampened diffusive model is rooted in early work in theoretical morphology that focused on the constrained filling of morphospace (Raup 1968).

The simulated diffusions and empirical observation of evolutionary enablers hint at the source of teleological concepts in human evolution. If the morphological and neurological traits can be assumed to have followed a multivariate Markovian diffusion that is at least qualitatively similar to the simulations in Figure 4 (especially Fig. 4a), the pattern in evolutionary rates along the path leading to humans may paint a misleading view that such changes have followed a progressive trend leading to a human-defined apex. However, the mosaic analysis here suggests that humans' biological uniqueness can be attributed to a relatively small number of anatomical rearrangements built over a longer diffusion into an area of developmental-morphospace occupied by all apes that is characterized by increased structural opportunity. Instead of treating humans as exceptional, this view suggests that the structural opportunities that emerged early in ape evolution may have freed the ancestors of currently extant taxa to blaze unique trajectories along a complex, multivariate adaptive landscape that would have been otherwise inaccessible. Structurally, all ape species might therefore be viewed as equally progressive in their evolution, with species-level differences in form and function shaped by stochastic differences in separate realized evolutionary paths along a shared adaptive landscape. Alternatively, separate taxa may have forged new and unique adaptive

landscapes following speciation events as structural differences between newly isolated species drove the creation of new functional niches early in hominoid evolution.

The empirical and simulated analyses presented here are consistent with, although do not provide independent support for, a picture of morphological evolution that involves episodic diffusion across adaptive zones. However, the empirical and theoretical analyses allow for alternating and interacting roles for both ecological and constructional opportunity. This view can supplement many existing conceptions of adaptive radiation and key innovation by providing an alternative to ecological opportunity as a lone driving factor in the disparification of form. Instead, phenotypic disparity produced through diffusion into a set of abundant adaptive zones can be directed and limited by the availability of structural opportunity. Nature surely merges these simplified extremes when shaping patterns in biodiversity (Seilacher 1991), and so increased emphasis on the interplay between ecological, developmental, and constructional factors will be a critical part of shaping a pluralistic understanding of the complex patterns and processes that have shaped the vast diversity across the tree of life.

Funding

This work was carried out while the author was funded by a Predoctoral Fellowship provided by the Rackham Graduate School at the University of Michigan.

Acknowledgements

I wish to thank D Alvarado-Serrano, M Cosman, CW Dick, DC Fisher, LM MacLatchy, H Marx, J Saulsbury, SA Smith, N Walker-Hale for conversations that have greatly benefitted this work. I also thank S Worthington for help accessing the skeletal measurements that comprised much of the character matrix analyzed here.

References

Andrews P. 1992 Evolution and environment in the Hominoidea. Nature 360, 641–646. (doi:10.1038/360641a0)

Berge C. 1998 Heterochronic processes in human evolution: An ontogenetic analysis of the hominid pelvis. American Journal of Physical Anthropology 105, 441–459. (doi:10.1002/(sici)1096-8644(199804)105:4<441::aid-ajpa4>3.0.co;2-r)

Boddy AM, McGowen MR, Sherwood CC, Grossman LI, Goodman M, Wildman DE. 2012 Comparative analysis of encephalization in mammals reveals relaxed constraints on anthropoid primate and cetacean brain scaling. Journal of Evolutionary Biology 25, 981–994. (doi:10.1111/j.1420-9101.2012.02491.x)

Bouckaert R, Heled J, Kühnert D, Vaughan T, Wu C-H, Xie D, Suchard MA, Rambaut A, Drummond AJ. 2014 BEAST 2: A Software Platform for Bayesian Evolutionary Analysis. PLoS Computational Biology 10, e1003537. (doi:10.1371/journal.pcbi.1003537)

Capellini I, Venditti C, Barton, RA. 2010 Phylogeny and metabolic scaling in mammals. Ecology, 91, 2783-2793.

Charlesworth B, Lande R, Slatkin M. 1982 A Neo-Darwinian Commentary on Macroevolution. Evolution 36, 474–498. (doi:10.1111/j.1558-5646.1982.tb05068.x)

Cheverud JM. 1984 Quantitative genetics and developmental constraints on evolution by selection. Journal of Theoretical Biology 110, 155–171. (doi:10.1016/s0022-5193(84)80050-8)

Crouch NMA, Ricklefs RE. 2019 Speciation Rate Is Independent of the Rate of Evolution of Morphological Size, Shape, and Absolute Morphological Specialization in a Large Clade of Birds. The American Naturalist 193, E78–E91. (doi:10.1086/701630)

Donoghue MJ, Ree RH. 2000 Homoplasy and Developmental Constraint: A Model and an Example from Plants. American Zoologist 40, 759–769. (doi:10.1093/icb/40.5.759)

Donoghue MJ. 2005 Key innovations, convergence, and success: macroevolutionary lessons from plant phylogeny. Paleobiology 31, 77-93. (doi: 10.1666/0094-8373(2005)031[0077:KICASM]2.0.CO;2)

Felice RN, Goswami A. 2017 Developmental origins of mosaic evolution in the avian cranium. Proceedings of the National Academy of Sciences 115, 555–560. (doi:10.1073/pnas.1716437115)

Fisher, DC. 1986 Progress in organismal design. Pp. 99-117 in: Patterns and Processes in the History of Life. Raup DM and Jablonski D, eds. Springer, Berlin, Heidelberg.

Goswami A, Binder WJ, Meachen J, O'Keefe FR. 2015 The fossil record of phenotypic integration and modularity: A deep-time perspective on developmental and evolutionary dynamics. Proceedings of the National Academy of Sciences 112, 4891–4896. (doi:10.1073/pnas.1403667112)

Goswami A, Smaers JB, Soligo C, Polly PD. 2014 The macroevolutionary consequences of phenotypic integration: from development to deep time. Philosophical

Transactions of the Royal Society B: Biological Sciences 369, 20130254–20130254. (doi:10.1098/rstb.2013.0254)

Gould SJ, Vrba ES. 1982 Exaptation—a Missing Term in the Science of Form. Paleobiology 8, 4–15. (doi:10.1017/s0094837300004310)

Gould SJ and Lewontin RC. 1979 The spandrels of San Marco and the Panglossian paradigm: a critique of the adaptationist programme. Proceedings of the Royal Society of London. Series B. Biological Sciences 205, 581–598. (doi:10.1098/rspb.1979.0086)

Gould, SJ. 1977 Ontogeny and Phylogeny. Harvard University Press, Cambridge, USA.

Harmon LJ. 2003 Tempo and Mode of Evolutionary Radiation in Iguanian Lizards. Science 301, 961–964. (doi:10.1126/science.1084786)

Holloway RL. 1973 Endocranial volumes of early African hominids, and the role of the brain in human mosaic evolution. Journal of Human Evolution 2, 449–459. (doi:10.1016/0047-2484(73)90123-1)

Hunt KD. 2016 Why are there apes? Evidence for the co-evolution of ape and monkey ecomorphology. Journal of Anatomy 228, 630–685. (doi:10.1111/joa.12454)

Lewton KL. 2010 Locomotor function and the evolution of the primate pelvis. (Doctoral dissertation, Arizona State University).

Losos JB. 2010 Adaptive Radiation, Ecological Opportunity, and Evolutionary Determinism. The American Naturalist 175, 623–639. (doi:10.1086/652433)

Mahler DL, Ingram T, Revell LJ, Losos JB. 2013 Exceptional Convergence on the Macroevolutionary Landscape in Island Lizard Radiations. Science 341, 292–295. (doi:10.1126/science.1232392)

McHenry H. 1975 Fossils and the mosaic nature of human evolution. Science 190, 425–431. (doi:10.1126/science.809842)

Michel LA et al. 2014 Remnants of an ancient forest provide ecological context for Early Miocene fossil apes. Nature Communications 5. (doi:10.1038/ncomms4236)

Rice, SH. 2002. The role of heterochrony in primate brain evolution. In: Human evolution through developmental change. N. Minugh-Purvis & K.J. McNamara, eds. Johns Hopkins Univ. Press, Baltimore.

Seilacher A. 1991 Self-Organizing Mechanisms in Morphogenesis and Evolution. In Constructional Morphology and Evolution, pp. 251–271. Springer Berlin Heidelberg. (doi:10.1007/978-3-642-76156-0_17)

Smith JM, Burian R, Kauffman S, Alberch P, Campbell J, Goodwin B, Lande R, Raup D, Wolpert L. 1985 Developmental Constraints and Evolution: A Perspective from the Mountain Lake Conference on Development and Evolution. The Quarterly Review of Biology 60, 265–287. (doi:10.1086/414425)

Olson ME. 2012 The developmental renaissance in adaptationism. Trends in Ecology and Evolution 27, 278–287. (doi:10.1016/j.tree.2011.12.005)

Olson EC and Miller RL. 1999. Morphological Integration. University of Chicago Press.

Parins-Fukuchi C. 2018 Bayesian placement of fossils on phylogenies using quantitative morphometric data. Evolution 72, 1801–1814. (doi:10.1111/evo.13516)

Parins-Fukuchi C. 2018 Detecting mosaic patterns in phenotypic disparity. *bioRxiv*, 423228.

Rabosky DL, Santini F, Eastman J, Smith SA, Sidlauskas B, Chang J, Alfaro ME. 2013 Rates of speciation and morphological evolution are correlated across the largest vertebrate radiation. Nature Communications 4. (doi:10.1038/ncomms2958)

Rabosky DL. 2014 Automatic Detection of Key Innovations, Rate Shifts, and Diversity-Dependence on Phylogenetic Trees. PLoS One 9, e89543. (doi:10.1371/journal.pone.0089543)

Rabosky DL, Grundler M, Anderson C, Title P, Shi JJ, Brown JW, Huang H, Larson JG. 2014 BAMMtools: an R package for the analysis of evolutionary dynamics on phylogenetic trees. Methods in Ecology and Evolution 5, 701–707. (doi:10.1111/2041-210x.12199)

Rainey PB, Travisano M. 1998 Adaptive radiation in a heterogeneous environment. Nature 394, 69–72. (doi:10.1038/27900)

Raup DM. 1968 Theoretical morphology of echinoid growth. Journal of Paleontology 42, 50-63.

Ruff CB. 1994 Morphological adaptation to climate in modern and fossil hominids. American Journal of Physical Anthropology 37, 65–107. (doi:10.1002/ajpa.1330370605)

Simpson GG. 1944 Tempo and Mode in Evolution. Columbia University Press. New York.

Slater GJ, Friscia AR. 2019 Hierarchy in adaptive radiation: A case study using the Carnivora (Mammalia). Evolution 73, 524–539. (doi:10.1111/evo.13689)

Slater GJ. 2015 Iterative adaptive radiations of fossil canids show no evidence for diversity-dependent trait evolution. Proceedings of the National Academy of Sciences 112, 4897–4902. (doi:10.1073/pnas.1403666111)

Sukumaran J, Holder MT. 2010 DendroPy: a Python library for phylogenetic computing. Bioinformatics 26, 1569–1571. (doi:10.1093/bioinformatics/btq228)

Stebbins GL. 1983 Mosaic evolution: An integrating principle for the modern synthesis. Experientia 39, 823–834. (doi:10.1007/bf01990398)

Stebbins GL. 1984 Mosaic evolution, mosaic selection and angiosperm phylogeny. Botanical Journal of the Linnean Society 88, 149–164. (doi:10.1111/j.1095-8339.1984.tb01568.x)

Vos RA. 2006 Inferring large phylogenies: the big tree problem (Doctoral dissertation, Simon Fraser University)

Waddington CH. 1959 Canalization of Development and Genetic Assimilation of Acquired Characters. Nature 183, 1654–1655. (doi:10.1038/1831654a0)

Wagner CE, Harmon LJ, Seehausen O. 2012 Ecological opportunity and sexual selection together predict adaptive radiation. Nature 487, 366–369. (doi:10.1038/nature11144)

Wagner GP, Amemiya C, Ruddle F. 2003 Hox cluster duplications and the opportunity for evolutionary novelties. Proceedings of the National Academy of Sciences 100, 14603–14606. (doi:10.1073/pnas.2536656100)

Wagner GP. 1988 The influence of variation and of developmental constraints on the rate of multivariate phenotypic evolution. Journal of Evolutionary Biology 1, 45–66. (doi:10.1046/j.1420-9101.1988.1010045.x)

Wagner PJ. 2018 Early bursts of disparity and the reorganization of character integration. Proceedings of the Royal Society B: Biological Sciences 285, 20181604. (doi:10.1098/rspb.2018.1604)

Worthington S. 2012 New approaches to late Miocene hominoid systematics: Ranking morphological characters by phylogenetic signal (Doctoral dissertation, New York University).

Yoder JB, et al. 2010 Ecological opportunity and the origin of adaptive radiations. Journal of Evolutionary Biology 23, 1581–1596. (doi:10.1111/j.1420-9101.2010.02029.x)

Young NM, Wagner GP, Hallgrímsson B. 2010 Development and the evolvability of human limbs. Proceedings of the National Academy of Sciences 107, 3400–3405. (doi:10.1073/pnas.0911856107)

Figures

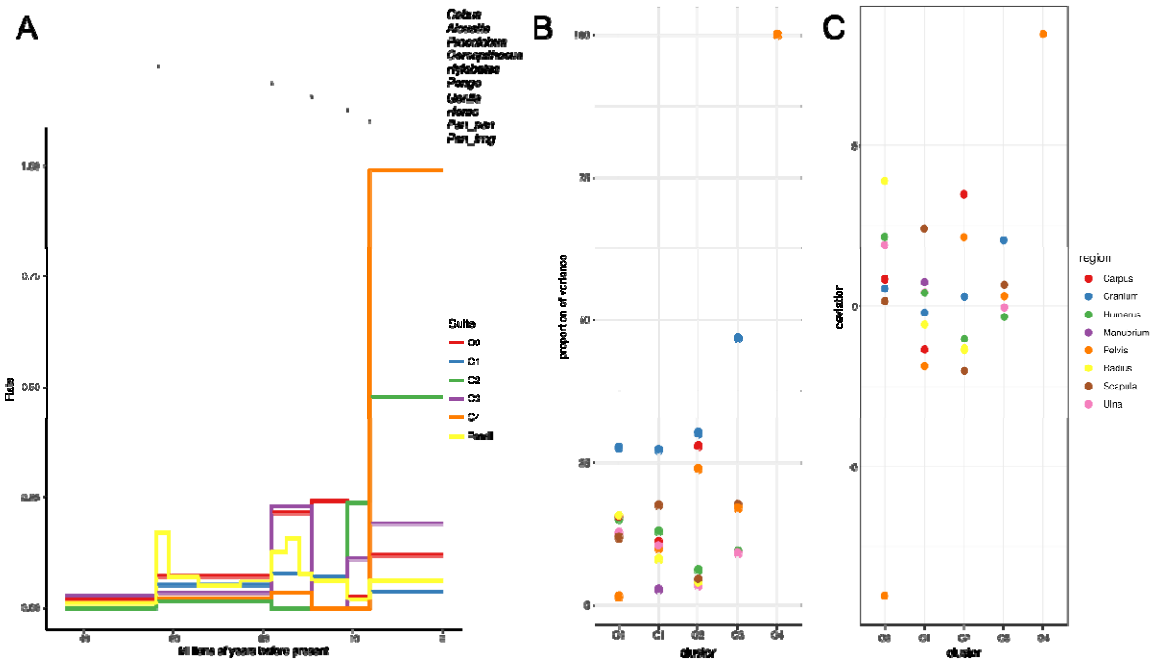

Figure 1. A) Mosaic evolutionary rates across extant catarrhines. B) Variance contributed to each suite by each skeletal region, estimated from a principal component analysis. C) Skeletal regions over-represented in each mosaic evolutionary suite. Values above zero correspond to regions that occupy a higher proportion of their clusters than expected.

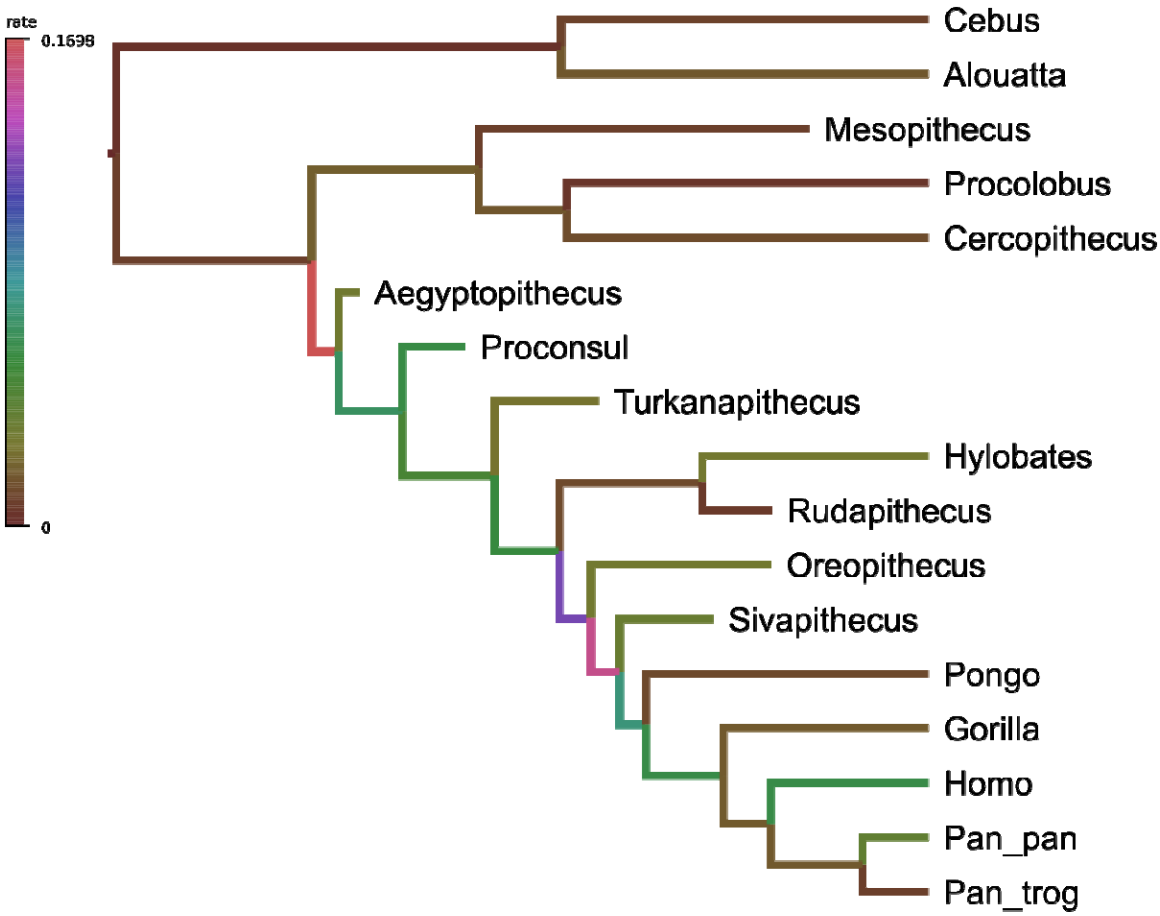

Figure 2. Placements of fossil genera on extant reference tree. Branch colors correspond to evolutionary rate along individual branches.

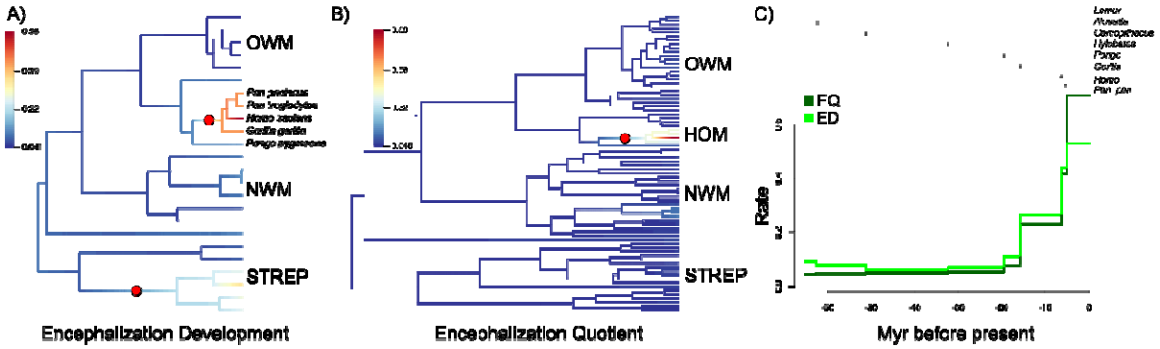

Figure 3. Rate shifts in A) encephalization development, and B) encephalization quotient. C) Branch-specific evolutionary rates when tracing the lineage from *Homo* to the root.

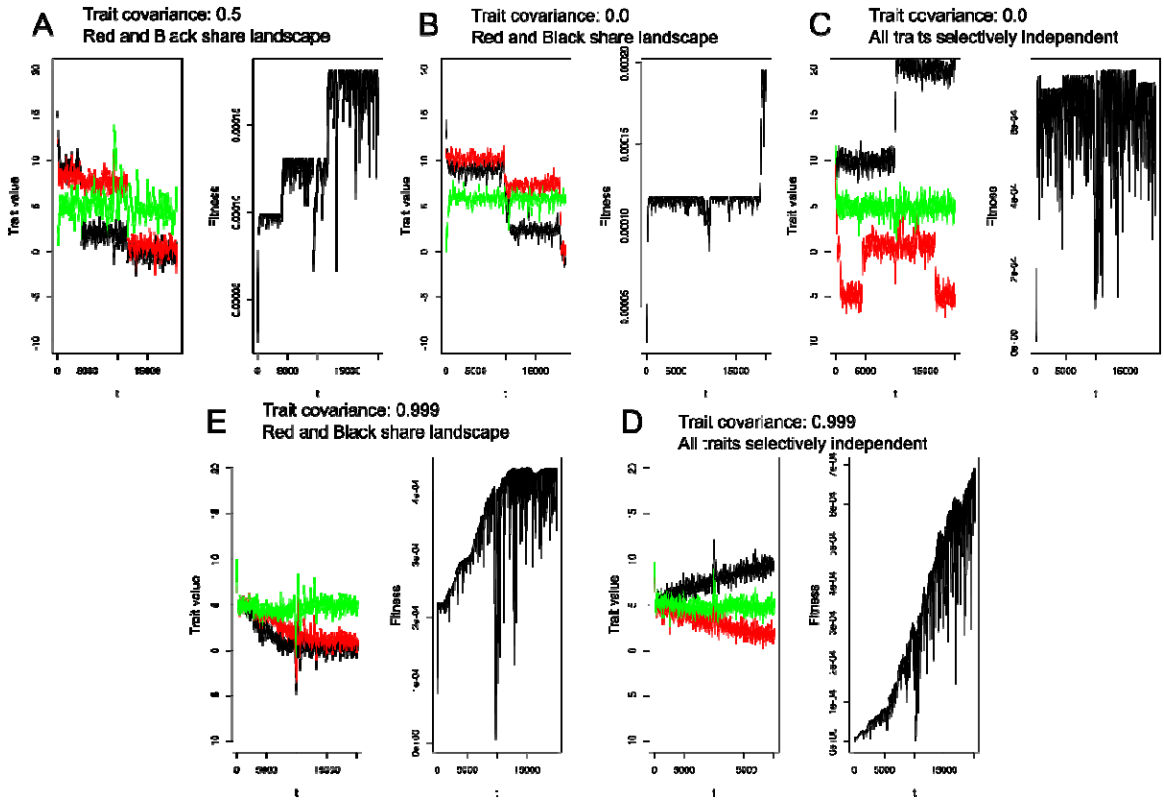

Figure 4. Monte Carlo simulations of integrated and atomized systems of three continuous traits. Each box is a simulated diffusion between three traits under A) moderate developmental linkage and shared selection, B) no developmental linkage and shared selection, C) no developmental linkage and selective independence, D) high developmental linkage and selective independence, and E) high developmental linkage and shared selection.

suite	skeletal region	trait
0	Ulna	Olecranon length
0	Ulna	Middle shaft shape
0	Ulna	Olecranon shape
0	Ulna	Distal shape
0	Ulna	Styloid process length
0	Ulna	Proximal shaft shape
0	Ulna	Coronoid
0	Ulna	Trochlea notch shape
0	Humerus	Head P D shape
0	Humerus	Trochlea
0	Humerus	Intertubercular angle
0	Humerus	Lat. trochlea keel dev.
0	Humerus	Bicipital groove shape
0	Humerus	Humeral Head Size
0	Humerus	Head torsion
0	Humerus	Trochlea sup. notch angle
0	Humerus	Zona conoidea dist. depth
0	Humerus	Grt. tuberosity proj.
0	Carpus	Capitate head M L width
0	Carpus	Capitate M C 3 shape
0	Carpus	CAPCM4
0	Carpus	Hamate DP depth COR
0	Carpus	Capitate head A P / P D
0	Carpus	Capitate dorsal nonarticular
0	Carpus	Capitate M C 3 depth
0	Carpus	Lunate dist.

0 Carpus	Hamate triquetral facet angle
0 Carpus	Capitate M C 2 facets
0 Cranium	Grt. palatine foramen position
0 Cranium	Zygomatic root origin elevation
0 Cranium	Basicranial length
0 Cranium	Piriform aperture shape
0 Cranium	Postglenoid projection
0 Cranium	Basicranium vs. palate
0 Cranium	Bregma position
0 Cranium	Lacrimal fossa & orbital floor
0 Cranium	Facial projection
0 Cranium	Zygomax. tubercle A P width
0 Cranium	Basicranium vs. nuchal
0 Cranium	Nasoalveolar clivus length
0 Cranium	Head M L shape
0 Cranium	Zygomatic
0 Cranium	Face height vs. depth
0 Cranium	Piriform max. M L elevation
0 Cranium	Neurocranial shape
0 Cranium	Asterion angle
0 Radius	Lunate facet shape
0 Radius	Lunate facet angle
0 Radius	Neck shape
0 Radius	Scapholunate facet areas
0 Radius	Lunate facet dorsal proj.
0 Radius	Distal facets area
0 Radius	Total length

0 Radius	Radial neck length
0 Radius	Shaft curvature M L
0 Radius	Head articular surface P D
0 Scapula	Trapezius insert angle
0 Scapula	Coraco
0 Scapula	Inf. glenoid cor
0 Scapula	Acromian size
0 Scapula	Inferior angle
0 Scapula	Sup. notch shape
0 Scapula	Spinatus ratio
0 Scapula	Glenoid vent. bar angle
0 Pelvis	pubic symphysis length
1 Ulna	Ulna head height
1 Ulna	Semilunar keel angle
1 Ulna	Radial notch shape
1 Ulna	Distal shaft shape
1 Humerus	Dist. articular shape
1 Humerus	Trochlea dist. waisting
1 Humerus	Med. trochlea keel dev.
1 Humerus	Olecranon fossa depth
1 Humerus	Olecranon fossa shape
1 Carpus	Capitate P D length
1 Carpus	Hamate M C 4
1 Carpus	Lunate radial facet M L
1 Carpus	Lunate triquetral facet shape
1 Cranium	Piriform base M L width
1 Cranium	M1 shape

1 Cranium	Lsr. palatine foramen
1 Cranium	Molar crown areas
1 Cranium	Entoglenoid width
1 Cranium	Entoglenoid projection
1 Cranium	Nasal bone M L width
1 Cranium	Orbital margin M L width
1 Cranium	Orbit area
1 Cranium	Interorbital width
1 Radius	Distal surface shape
1 Radius	Styloid process length
1 Radius	Radial Head Shape
1 Manubrium	Manubrium shape
1 Scapula	Scapula Body shape
1 Scapula	Trapezius med. insert
1 Scapula	Superior angle
1 Scapula	Subscapular depth
1 Scapula	Vertebral border length
1 Scapula	Glenoid fossa shape
1 Scapula	Coracoid length
1 Pelvis	illium length
1 Pelvis	bi
1 Pelvis	anteroposterior pelvic diameter
1 Pelvis	pelvic length
2 Humerus	Epicondyles projection
2 Humerus	Olecranon perforation
2 Ulna	Shaft curvature A P
2 Carpus	Capitate M C 3 waisting

2 Carpus	Capitate waisting
2 Carpus	Lunate PD Length
2 Carpus	Hamate hamulus P D proj.
2 Carpus	Capitate M C 2 margin
2 Carpus	Capitate M C 2 orientation
2 Carpus	Lunate dist. facet shape
2 Cranium	Orbit shape
2 Cranium	Pterion post. config
2 Cranium	Palate shape
2 Cranium	Lacrimal fossa visibility
2 Cranium	Palatine width
2 Cranium	Postorbital constriction
2 Cranium	Palate depth
2 Radius	Head depth P D
2 Scapula	Glenoid fossa depth
2 Pelvis	illium width
2 Pelvis	ischium length
2 Pelvis	AIIS to hip joint
2 Pelvis	inferior pubic ramus length
2 Pelvis	acetabulum diameter
2 Pelvis	superior pubic ramus length
3 Scapula	Spinoglenoid notch depth
3 Scapula	Infraglenoid tuberosity M L
3 Pelvis	lower illiac height
3 Pelvis	inferior pubic ramus cross
3 Ulna	Radial notch depth
3 Cranium	Temporal fossa width

3 Cranium	Face vs. nasal height
3 Cranium	Face height vs. width
3 Cranium	Palate width
3 Cranium	Entoglenoid lat. pterygoid
3 Humerus	Medial trochlea keel & medial epicon
4 Pelvis	ischium cross
4 Pelvis	superior pubic ramus cross
4 Pelvis	upper illiac height
4 Pelvis	lower ilium cross
4 Pelvis	ischium dorsal projection
4 Pelvis	pubic symphysis
4 Pelvis	auricular surface area
4 Pelvis	biacetabular diameter
4 Pelvis	maximum transverse diameter
4 Pelvis	sacrum width

Table S1: List of traits and their skeletal regions that comprise each of the mosaic suites detected from the skeletal data.